

Ferromagnetic Resonance in Metal Single Crystals*

J. O. ARTMAN

Gordon McKay Laboratory, Harvard University, Cambridge, Massachusetts

(Received July 27, 1956)

Microwave susceptibility expressions for ferromagnetic resonance have been derived for metal single crystals possessing crystalline anisotropy. Crystals of uniaxial and cubic magnetic symmetry are considered. When the magnetization \mathbf{M} is aligned with the applied field \mathbf{H} , the results are equivalent to those of Kittel. When a simple multidomain structure occurs on a crystal face, two resonances are found for a given H . These correspond to microwave excitation being perpendicular or parallel to \mathbf{H} . These multidomain resonances are related to H , saturation magnetization M , anisotropy parameter K/M , and the ratio of skin-depth to domain width. Thus domain spacings can be inferred from microwave measurements. In particular, predictions of the theory are compared with the microwave measurements of Kip and Arnold and magnetic domain pattern observations in the literature. Secondary resonances found in Ni by Reich can also be attributed to a multidomain structure.

I. INTRODUCTION

THE tensorial properties of conducting ferromagnetic media have been used by Young and Uehling¹ to describe resonance phenomena observed in microwave cavities. The Young and Uehling derivations were given for microwave magnetic susceptibilities of the form

$$\begin{pmatrix} \chi & -j\kappa & 0 \\ j\kappa & \chi & 0 \\ 0 & 0 & 0 \end{pmatrix}, \quad (1)$$

but can be generalized immediately to susceptibilities of the less restrictive form

$$\begin{pmatrix} \chi_{11} & -j\kappa_{12} & 0 \\ j\kappa_{21} & \chi_{22} & 0 \\ 0 & 0 & \chi_{33} \end{pmatrix}. \quad (2)$$

Derivations of the ferromagnetic resonance relations applicable to single crystals with magnetic anisotropy have been given recently by Smit and Beljers,² Zeiger,³ and Suhl.⁴ Extensions to simple multidomain configurations have been given by Smit and Beljers,² Nagamiya,⁵ and by Artman.⁶ The above analyses refer to nonconducting ferromagnetic substances for which propagation-depth effects are usually ignored so that the dc and rf demagnetizing factors are the same. In this paper we will modify the analyses so as to apply to conducting ferromagnetic media. Formulas will be given for crystals of cubic and uniaxial magnetic symmetry.

The susceptibility tensor derivation follows from

* The research in this document was supported by the U. S. Air Force under contract with Harvard University.

¹ J. A. Young, Jr. and E. A. Uehling, Phys. Rev. **94**, 544 (1954).

² J. Smit and H. G. Beljers, Philips Research Repts. **10**, 113 (1955).

³ H. J. Zeiger, Lincoln Laboratory (private communication).

⁴ H. Suhl, Phys. Rev. **97**, 555 (1955).

⁵ T. Nagamiya, Progr. Theoret. Phys. (Japan) **10**, 72 (1953).

⁶ J. O. Artman, Phys. Rev. **100**, 1243(A) (1955), Proc. Inst. Radio Engrs. **44**, No. 10, 1284 (1956); Phys. Rev. **105**, 62 (1957), preceding paper.

examination of the free energy. First, orientation of the magnetization \mathbf{M} necessary for static equilibrium in the presence of a dc magnetic field \mathbf{H} is determined. The tensor susceptibility components (2) are then evaluated from consideration of small gyrations of \mathbf{M} about the equilibrium direction. The propagation relations and the cavity perturbation equations are next obtained by the procedure of Young and Uehling. When the crystal is a single magnetic domain and \mathbf{H} is applied along a principal direction, the results are equivalent to those derived first by Kittel.⁷ Simple structures in which the crystal is composed of many magnetic domains are also considered. Observations made by Kip and Arnold⁸ in Fe, by Reich⁹ in Ni, and by Ohtsuka¹⁰ in Co are compared with theory.

II. SINGLE-DOMAIN ANALYSIS

(a) Cubic Crystal-Disk in (01 $\bar{1}$) Plane

Consider a thin disk lying in a (01 $\bar{1}$) plane as shown in Fig. 1. \mathbf{H} lies in this plane and is inclined at the angle ψ to the [100] axis. \mathbf{M} is inclined to the [100] axis at the angle θ . The azimuth of \mathbf{M} with respect to the [010] axis is ϕ . The free energy per unit volume, considering just first-order anisotropy and magnetic contributions, is

$$\begin{aligned} F = & \frac{1}{4} K_1 [\sin^2(2\theta) + \sin^4\theta \sin^2(2\phi)] \\ & - MH [\cos\theta \cos\psi + \sin\theta \sin\psi \sin(\frac{1}{4}\pi + \phi)] \\ & + \frac{1}{2} \times 4\pi M^2 [n \cos^2\theta + n \sin^2\theta \sin^2(\frac{1}{4}\pi + \phi) \\ & + (1 - 2n) \sin^2\theta \cos^2(\frac{1}{4}\pi + \phi)], \quad (3) \end{aligned}$$

where K_1 is the first-order anisotropy energy constant and $4\pi n$ is the demagnetization factor in the plane of

⁷ C. Kittel, Phys. Rev. **73**, 155 (1948).

⁸ A. F. Kip and R. D. Arnold, Phys. Rev. **75**, 1556 (1949).

⁹ K. H. Reich, Phys. Rev. **101**, 1647 (1956) and private communication.

¹⁰ T. Ohtsuka, Technical Report No. 187, Cruft Laboratory, Harvard University, August 30, 1953 (unpublished).

the disk. The angular derivatives of the free energy are

$$\begin{aligned} \partial F/\partial\phi = & \frac{1}{4}K_1[2\sin 4\phi\sin^4\theta] \\ & - MH\sin\theta\sin\psi\cos(\frac{1}{4}\pi+\phi) \\ & - 2\pi M^2(1-3n)\sin^2\theta\sin(\frac{1}{2}\pi+2\phi), \quad (4) \end{aligned}$$

$$\begin{aligned} \partial F/\partial\theta = & \frac{1}{4}K_1[2\sin 4\theta+4\sin^3\theta\cos\theta\sin^2(2\phi)] \\ & - MH[-\sin\theta\cos\psi+\cos\theta\sin\psi\sin(\frac{1}{4}\pi+\phi)] \\ & + 2\pi M^2[-n\sin 2\theta+n\sin 2\theta\sin^2(\frac{1}{4}\pi+\phi) \\ & + (1-2n)\sin 2\theta\cos^2(\frac{1}{4}\pi+\phi)]. \end{aligned}$$

At equilibrium, $\partial F/\partial\theta = \partial F/\partial\phi = 0$. These relations are satisfied by $\phi = \frac{1}{4}\pi$ and the equation

$$MH\sin(\psi-\theta) = K_1\sin\theta\cos\theta(3\cos^2\theta-1). \quad (5)$$

Lineup of \mathbf{M} with \mathbf{H} can occur only for roots of the equation $\sin\theta\cos\theta(3\cos^2\theta-1) = 0$, namely, $\theta = 0, \pi/2, \cos^{-1}\sqrt{1/3}$.

To evaluate the tensor components and resonance relations, second-order derivatives must be calculated. Since the rf fields are confined to a very small depth, the effects of dynamic demagnetizing fields in the plane of the metal can be ignored. The rf demagnetizing fields perpendicular to the plane of the disk do not enter as such but will be accounted for later by the boundary conditions at the metal-air interface. We consider a thin lamina in the interior of the specimen parallel to the plane of the disk. In Eqs. (4) \mathbf{H} is replaced by the internal field \mathbf{H}' , where $\mathbf{H}' = \mathbf{H} - 4\pi\mathbf{M}n$. The angle ψ between the $[100]$ axis and \mathbf{H} is replaced by ψ' , the angle between the $[100]$ axis and \mathbf{H}' . The demagnetization term involving M^2 is dropped. The second-order derivatives of these modified equations evaluated at $\phi = \pi/4$ are

$$\begin{aligned} \partial^2 F'/\partial\theta^2 = & K_1[12\sin^4\theta - 13\sin^2\theta + 2] \\ & + MH'\cos(\psi'-\theta), \quad (6) \end{aligned}$$

$$\partial^2 F'/\partial\phi^2 = 2K_1\sin^4\theta + MH'\sin\theta\sin\psi',$$

$$\partial^2 F'/\partial\theta\partial\phi = 0.$$

F has been replaced by F' in these equations. The resonant angular frequency ω' follows from the equation²⁻⁴:

$$\frac{\omega'}{\gamma} = \frac{1}{M\sin\theta} \left[\frac{\partial^2 F'}{\partial\theta^2} \frac{\partial^2 F'}{\partial\phi^2} - \left(\frac{\partial^2 F'}{\partial\theta\partial\phi} \right)^2 \right]^{\frac{1}{2}}, \quad (7)$$

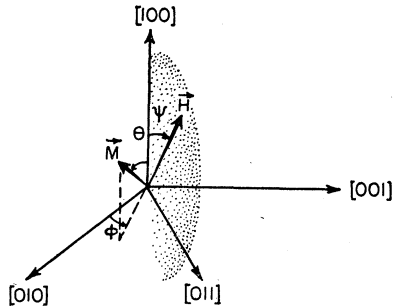


FIG. 1. \mathbf{M} and \mathbf{H} in cubic crystal, disk and \mathbf{H} in $(01\bar{1})$ plane.

where γ is the gyromagnetic ratio. Axes (1,2,3) are selected: (1) normal to \mathbf{M} and in the plane of the disk; (2) perpendicular to the plane of the disk; (3) parallel to \mathbf{M} . With reference to this system the susceptibility tensor elements are:

$$\begin{aligned} \chi_{11} = & \frac{4\pi M}{D} \left(\frac{1}{M\sin^2\theta} \frac{\partial^2 F'}{\partial\phi^2} \right), \\ \chi_{22} = & \frac{4\pi M}{D} \left(\frac{1}{M} \frac{\partial^2 F'}{\partial\theta^2} \right), \quad (8) \end{aligned}$$

$$j\kappa_{12} = j\kappa_{21} = j\kappa = \frac{4\pi M}{D} \left(j\frac{\omega_0}{\gamma} + \frac{1}{\gamma T} \right),$$

where

$$D = \frac{\omega'^2}{\gamma^2} - \frac{\omega_0^2}{\gamma^2} + \frac{1}{\gamma^2 T^2} + j\frac{2\omega_0}{\gamma T}, \quad (9)$$

in which ω_0 is the microwave angular frequency and $1/\gamma T$ the ferromagnetic resonance breadth. Young and Uehling have considered plane wave propagation in metals whose magnetic properties are specified by the tensor (1). As shown in the Appendix, their formulation can be carried over to media specified by the more general tensor (2). For rf propagation in direction 2 and surface excitation in direction 1, the perturbation on the cavity is

$$\begin{aligned} \Delta \left(\frac{1}{Q} \right) - 2j \frac{\Delta\omega_0}{\omega_0} = & \left(\frac{c^2}{4\pi\omega_0\sigma} \right)^{\frac{1}{2}} \\ & \times \left[j \frac{(1+\chi_{11})(1+\chi_{22}) - \kappa^2}{1+\chi_{22}} \right]^{\frac{1}{2}}, \quad (10) \end{aligned}$$

where σ is the conductivity. If, in (7) and (9), $(1/M\sin^2\theta)(\partial^2 F'/\partial\phi^2)$ is replaced by $(1/M\sin^2\theta)(\partial^2 F'/\partial\phi^2) + 4\pi M$, then the resulting expression for $1+\chi_{11}$ is found to be identical with $[(1+\chi_{11})(1+\chi_{22}) - \kappa^2]/(1+\chi_{22})$ in Eq. (10). Hence the perturbation of the cavity is governed by

$$\begin{aligned} \frac{(1+\chi_{11})(1+\chi_{22}) - \kappa^2}{1+\chi_{22}} = & 1 + \frac{4\pi M \left[\frac{1}{M\sin^2\theta} \frac{\partial^2 F'}{\partial\phi^2} + 4\pi M \right]}{\left(\frac{\omega}{\gamma} \right)^2 - \left(\frac{\omega_0}{\gamma} \right)^2 + \frac{1}{\gamma^2 T^2} + j\frac{2\omega_0}{\gamma T}}, \quad (11) \end{aligned}$$

with

$$\left(\frac{\omega}{\gamma} \right)^2 = \frac{1}{M} \frac{\partial^2 F'}{\partial\theta^2} \left[\frac{1}{M\sin^2\theta} \frac{\partial^2 F'}{\partial\phi^2} + 4\pi M \right]. \quad (12)$$

Situations in which \mathbf{M} is parallel, or almost parallel, to \mathbf{H} are frequently of interest. If the quantity $\psi - \theta \equiv \epsilon$

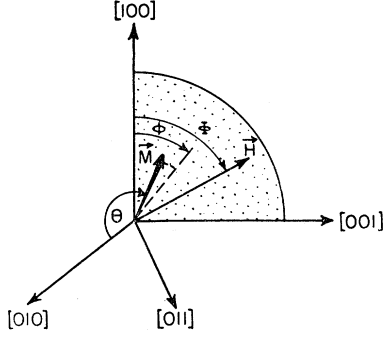


FIG. 2. \mathbf{M} and \mathbf{H} in cubic crystal, disk and \mathbf{H} in (010) plane.

becomes small,

$$\epsilon = \frac{K_1}{M} \times \frac{1}{H} \sin\theta \cos\theta (3 \cos^2\theta - 1). \quad (13)$$

To the first order in ϵ :

$$\begin{aligned} H' \cos(\psi' - \theta) &= H - 4\pi M n, \\ H' \sin\psi' / \sin\theta &= H + H\epsilon \cot\theta - 4\pi M n. \end{aligned} \quad (14)$$

Formulas (6) through (12) are modified accordingly. In particular, formula (12) becomes

$$\begin{aligned} \left(\frac{\omega}{\gamma}\right)^2 &= \left[\frac{K_1}{M} (12 \sin^4\theta - 13 \sin^2\theta) + H - 4\pi M n \right] \\ &\times \left[\frac{K_1}{M} (2 + 3 \sin^4\theta - 7 \sin^2\theta) + H + 4\pi M - 4\pi M n \right]. \end{aligned} \quad (15)$$

$$\begin{aligned} \text{At } \theta = 0: \quad \left(\frac{\omega}{\gamma}\right)^2 &= \left(\frac{2K_1}{M} + H - 4\pi M n \right) \\ &\times \left(\frac{2K_1}{M} + H + 4\pi M - 4\pi M n \right), \\ \theta = \cos^{-1}(\sqrt{\frac{1}{3}}): \quad \left(\frac{\omega}{\gamma}\right)^2 &= \left(\frac{4K_1}{3M} + H - 4\pi M n \right) \\ &\times \left(-\frac{4K_1}{3M} + H + 4\pi M - 4\pi M n \right), \\ \theta = \frac{\pi}{2}: \quad \left(\frac{\omega}{\gamma}\right)^2 &= \left(\frac{K_1}{M} + H - 4\pi M n \right) \\ &\times \left(-\frac{2K_1}{M} + H + 4\pi M - 4\pi M n \right). \end{aligned} \quad (16)$$

Equations (15) and (16) are the Kittel lineup formulas.

(b) Cubic Crystal-Disk in (010) Plane

The development is very similar to that of part (a). We now refer to Fig. 2. \mathbf{H} lies in the plane of the disk

and is inclined at the angle Φ to the $[100]$ axis. \mathbf{M} is inclined at the angle θ to the $[010]$ axis. The azimuth of \mathbf{M} with respect to the $[100]$ axis is ϕ . The expression for the free energy per unit volume is

$$\begin{aligned} F = & \frac{1}{4} K_1 [\sin^2(2\theta) + \sin^4\theta \sin^2(2\phi)] \\ & - MH [\sin\theta \cos(\Phi - \phi)] \\ & + \frac{1}{2} \times 4\pi M^2 [n \sin^2\theta + (1 - 2n) \cos^2\theta]. \end{aligned} \quad (17)$$

The equilibrium relations, $\partial F / \partial \theta = \partial F / \partial \phi = 0$, are satisfied by $\theta = \pi/2$ and

$$MH \sin(\Phi - \phi) = \frac{1}{2} K_1 \sin 4\phi. \quad (18)$$

\mathbf{M} can line up with \mathbf{H} only at ϕ values of 0 and $\frac{1}{4}\pi$. Analogously to (6) in part (a) we obtain

$$\begin{aligned} \frac{\partial^2 F'}{\partial \theta^2} &= K_1 [2 - \sin^2(2\phi)] + MH' \cos(\Phi' - \phi), \\ \frac{\partial^2 F'}{\partial \phi^2} &= 2K_1 \cos 4\phi + MH' \cos(\Phi' - \phi), \\ \frac{\partial^2 F'}{\partial \theta \partial \phi} &= 0, \end{aligned} \quad (19)$$

where Φ' is now the angle between the $[100]$ axis and \mathbf{H}' . With reference to axes (1,2,3) selected as in part (a) the susceptibility tensor elements are now

$$\begin{aligned} \chi_{11} &= \frac{4\pi M}{D} \left(\frac{1}{M} \frac{\partial^2 F'}{\partial \theta^2} \right), \\ \chi_{22} &= \frac{4\pi M}{D} \left(\frac{1}{M} \frac{\partial^2 F'}{\partial \phi^2} \right), \\ j\kappa_{12} = j\kappa_{21} = j\kappa &= \frac{4\pi M}{D} \left(j \frac{\omega_0}{\gamma} + \frac{1}{\gamma T} \right), \end{aligned} \quad (20)$$

where D is given by (9).

For rf excitation as in part (a), the expression $[(1 + \chi_{11})(1 + \chi_{22}) - \kappa^2] / (1 + \chi_{22})$ in (10) becomes

$$\begin{aligned} & 1 + \frac{4\pi M \left(\frac{1}{M} \frac{\partial^2 F'}{\partial \theta^2} + 4\pi M \right)}{\left(\frac{\omega}{\gamma}\right)^2 - \left(\frac{\omega_0}{\gamma}\right)^2 + \frac{1}{\gamma^2 T^2} + j \frac{2\omega_0}{\gamma T}}, \end{aligned} \quad (21)$$

where now

$$\left(\frac{\omega}{\gamma}\right)^2 = \left(\frac{1}{M} \frac{\partial^2 F'}{\partial \theta^2} + 4\pi M \right) \left(\frac{1}{M} \frac{\partial^2 F'}{\partial \phi^2} \right). \quad (22)$$

When the angle $\Phi - \phi \equiv \eta$ becomes small, then to first order in η

$$\eta = \frac{K_1}{M} \left(\frac{1}{H} \frac{\sin 4\phi}{2} \right), \quad (23)$$

$$H' \cos(\Phi' - \phi) = H - 4\pi M n.$$

Equation (22) becomes

$$\left(\frac{\omega}{\gamma}\right)^2 = \left(\frac{K_1}{M}(2 - \sin^2 2\phi) + H + 4\pi M - 4\pi Mn\right) \times \left(\frac{K_1}{M} 2 \cos 4\phi + H - 4\pi Mn\right). \quad (24)$$

$$\text{At } \phi = 0, \quad \left(\frac{\omega}{\gamma}\right)^2 = \left(\frac{2K_1}{M} + H + 4\pi M - 4\pi Mn\right) \times \left(2\frac{K_1}{M} + H - 4\pi Mn\right),$$

$$\text{At } \phi = \frac{\pi}{4}, \quad \left(\frac{\omega}{\gamma}\right)^2 = \left(\frac{K_1}{M} + H + 4\pi M - 4\pi Mn\right) \times \left(-\frac{2K_1}{M} + H - 4\pi Mn\right). \quad (25)$$

Equations (25) and (24) are the Kittel formulas.

(c) Uniaxial Crystal-Disk Containing Symmetry Axis [00·1]

We now refer to Fig. 3. \mathbf{H} lies in the plane of the disk and is inclined to the symmetry axis at the angle ψ . \mathbf{M} forms the angle θ with the symmetry axis and is inclined to the disk plane at the angle ϕ . The free energy per unit volume is

$$F = K_1 \sin^2 \theta - MH(\cos \theta \cos \psi + \sin \theta \sin \psi \cos \phi) + \frac{1}{2} \times 4\pi M^2 [n \cos^2 \theta + n \sin^2 \theta \cos^2 \phi + (1 - 2n) \sin^2 \theta \sin^2 \phi]. \quad (26)$$

The equilibrium relations, $\partial F / \partial \theta = \partial F / \partial \phi = 0$, are satisfied by $\phi = 0$ and

$$MH \sin(\psi - \theta) = K_1 \sin 2\theta. \quad (27)$$

Lineup of \mathbf{M} to \mathbf{H} can occur only for θ equal to 0 and $\frac{1}{2}\pi$. Corresponding to (6) in part (a), we obtain:

$$\begin{aligned} \partial^2 F' / \partial \theta^2 &= 2K_1 \cos 2\theta + MH' \cos(\psi - \theta), \\ \partial^2 F' / \partial \phi^2 &= MH' \sin \theta \sin \psi', \\ \partial^2 F' / \partial \theta \partial \phi &= 0, \end{aligned} \quad (28)$$

where ψ' is the angle between the symmetry axis and \mathbf{H}' . With reference to axes (1,2,3) selected as in part (a), the susceptibility elements are given by (8) and (9). Equations (10), (11), and (12) apply also. When the quantity $\psi - \theta \equiv \epsilon$ becomes small,

$$\epsilon = \frac{K_1}{M} \left(\frac{1}{H} \sin 2\theta \right). \quad (29)$$

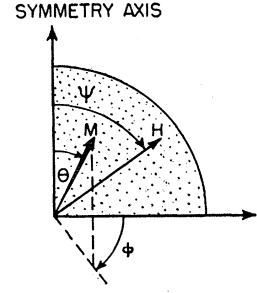


FIG. 3. \mathbf{M} and \mathbf{H} in uniaxial crystal, disk in plane containing symmetry axis. \mathbf{H} in plane of disk.

Relations (14) apply and the resonance formula (12) is

$$\left(\frac{\omega}{\gamma}\right)^2 = \left(\frac{K_1}{M}(2 \cos 2\theta) + H - 4\pi Mn\right) \times \left(\frac{K_1}{M}(2 \cos^2 \theta) + H + 4\pi M - 4\pi Mn\right). \quad (30)$$

$$\text{At } \theta = 0, \quad \left(\frac{\omega}{\gamma}\right)^2 = \left(\frac{2K_1}{M} + H - 4\pi Mn\right) \times \left(\frac{2K_1}{M} + H + 4\pi M - 4\pi Mn\right), \quad (31)$$

$$\text{At } \theta = \frac{\pi}{2}, \quad \left(\frac{\omega}{\gamma}\right)^2 = \left(-\frac{2K_1}{M} + H - 4\pi Mn\right) \times (H + 4\pi M - 4\pi Mn).$$

Equations (30) and (31) are the lineup formulas.

(d) Uniaxial Crystal-Disk Perpendicular to Symmetry Axis

Since none of the tensor elements is zero, the calculation for the general case cannot be treated by the simple methods given by Young and Uehling. Observations of Williams on cobalt reported by Bozorth¹¹ indicate that a simple one-domain structure does not exist at low magnetic fields; the general calculation therefore will not be attempted. However, if a magnetic field greater than $(2K_1/M) + 4\pi Mn$ is applied in the plane of the disk, then \mathbf{M} can line up with \mathbf{H} in stable equilibrium. Under these conditions the free energy per unit volume,

$$F = K_1 \sin^2 \theta - MH \sin \theta \cos \phi + \frac{1}{2} \times 4\pi M^2 [(1 - 2n) \cos^2 \theta + n \sin^2 \theta], \quad (32)$$

is in equilibrium at $\phi = 0$ and $\theta = \frac{1}{2}\pi$. Angles are defined as in (c) above. The second-order derivatives are

$$\begin{aligned} \partial^2 F' / \partial \theta^2 &= -2K_1 + M(H - 4\pi Mn), \\ \partial^2 F' / \partial \phi^2 &= M(H - 4\pi Mn), \\ \partial^2 F' / \partial \theta \partial \phi &= 0. \end{aligned} \quad (33)$$

¹¹ R. M. Bozorth, J. phys. radium 12, 308 (1951).

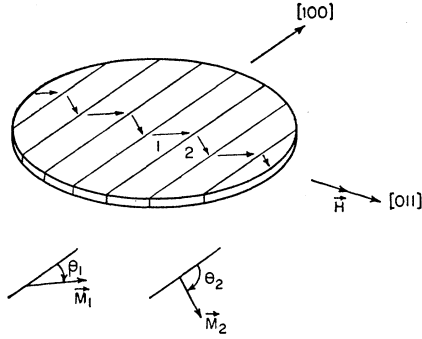


FIG. 4. Multidomain structure in cubic crystal of negative anisotropy. \mathbf{H} in $[011]$ direction of disk in $(01\bar{1})$ plane.

Relations (20) through (22) apply so that the resonance frequency observed for excitation perpendicular to \mathbf{H} and in the plane of the disk is given by

$$\left(\frac{\omega}{\gamma}\right)^2 = \left(-\frac{2K_1}{M} + H + 4\pi M(1-n)\right)(H - 4\pi Mn). \quad (34)$$

III. MULTIDOMAIN ANALYSIS

In Part II we have considered examples in which the direction of magnetization was constant throughout the specimen. Such simple structures frequently do not exist when the applied field is relatively small. Instead, patterns are found in which the crystal is composed of many magnetic domains—the direction of magnetization varying from domain to domain. As expected, these multidomain structures correspond to lower free energies than the single-domain structure. Fairly simple multidomain structures occur when \mathbf{H} is applied along certain of the principal directions. The theoretical and experimental situations have been reviewed recently by Stewart.¹² An earlier review was given by Kittel.¹³ In many instances the crystal is composed principally of an alternating sequence of just two varieties of domains. These two domain varieties correspond to two easy axes of magnetization being equally close to the direction of \mathbf{H} . The ferromagnetic resonances expected in such structures have been given for certain nonconducting crystals. Smit and Beljers² derived the relations for uniaxial $\text{BaFe}_{12}\text{O}_{19}$. Nagamiya⁵ considered the case of tetragonal symmetry and applied his results to observations on Fe_3O_4 made by Bickford. Artman⁶ has applied Smit's method to ferrite crystals of cubic symmetry. We shall consider the case of conducting ferromagnetic crystals in this section.

Cubic Crystals of Negative Anisotropy

(a) Disk in $(01\bar{1})$ Plane— \mathbf{H} in $[011]$ Direction

When a field \mathbf{H} of moderate strength is applied in the $[011]$ direction of a $(01\bar{1})$ crystal face we would

¹² K. H. Stewart, *Ferromagnetic Domains* (Cambridge University Press, Cambridge, 1954).

¹³ C. Kittel, *Revs. Modern Phys.* **21**, 541 (1949).

expect a magnetic structure to be essentially that of Fig. 4. The two types of domains correspond to magnetizations which tend to lie close to the two nearby body diagonals in the disk plane. The scale of the domain pattern is fixed by conditions at the boundaries of the specimen where the main domain structure is modified to avoid local demagnetizing fields. As described in references 12 and 13 these calculations involve consideration of additional domain wall energy and magnetostrictive energy terms in the free energy expression. In the derivations presented in this and subsequent sections we will regard the domain width as a fixed parameter. This domain width will be assumed constant throughout the specimen; the domains will be assumed to be equal in volume. The anisotropy and magnetostatic contributions of just the major domains to the free energy will be considered when calculating equilibrium and resonance conditions. Such a simplified treatment is adequate in accounting for the essential features of ferromagnetic resonance observed in a multidomain structure.

Accordingly, the free energy per unit volume, F , is

$$\begin{aligned} F = & \frac{1}{8}K_1[\sin^2(2\theta_1) + \sin^4\theta_1 \sin^2(2\phi_1) + \sin^2(2\theta_2) \\ & + \sin^4\theta_2 \sin^2(2\phi_2)] - \frac{1}{2}MH[\sin\theta_1 \sin(\frac{1}{4}\pi + \phi_1) \\ & + \sin\theta_2 \sin(\frac{1}{4}\pi + \phi_2)] + \frac{1}{2}\pi M^2\{n(\cos\theta_1 + \cos\theta_2)^2 \\ & + (1-2n)[\sin\theta_1 \cos(\frac{1}{4}\pi + \phi_1) + \sin\theta_2 \cos(\frac{1}{4}\pi + \phi_2)]^2 \\ & + n[\sin\theta_1 \sin(\frac{1}{4}\pi + \phi_1) + \sin\theta_2 \sin(\frac{1}{4}\pi + \phi_2)]^2\} \\ & + \frac{1}{2}\pi M^2 N[\sin\theta_1 \sin(\frac{1}{4}\pi + \phi_1) \\ & - \sin\theta_2 \sin(\frac{1}{4}\pi + \phi_2)]^2. \quad (35) \end{aligned}$$

The first term represents first-order anisotropy energy; the second, the magnetostatic interaction; the third, the demagnetization energy for the average magnetization on the surfaces of the specimen; and the fourth, the demagnetization energy of poles on the domain walls. The angle nomenclature corresponds to that used previously in Part II. For equilibrium, $\partial F/\partial\theta_1 = \partial F/\partial\theta_2 = \partial F/\partial\phi_1 = \partial F/\partial\phi_2 = 0$. These equations are satisfied by $\phi_1 = \phi_2 = \frac{1}{4}\pi$, $\theta = \theta_1 = \pi - \theta_2$, and

$$H = \left(-\frac{K_1}{M}(3 \sin^2\theta - 2) + 4\pi Mn\right) \sin\theta. \quad (36)$$

Since the applied field \mathbf{H} and the average magnetization are collinear, the internal field $H' = H - 4\pi Mn \sin\theta = (3 \sin^2\theta - 2) |K_1/M|$.

To evaluate the higher order derivatives we proceed as in Part II. H is replaced by H' and derivatives of the surface demagnetization term are dropped entirely. The dynamic demagnetizing fields on the domain walls, however, do contribute to these derivatives. We shall assume that the static demagnetizing factor N can be replaced by a dynamic demagnetizing factor N' . N' can be approximated from the static solution for an ellipsoid whose axes are proportional to domain length, domain width, and skin depth. Smit² has shown that

the oscillating charges on the domain walls couple the gyroscopic precession of the magnetizations in such a way that two resonant frequencies are found for a given H . These correspond to microwave excitation parallel or perpendicular to the domain walls. In our notation, the formulas of Smit are:

$$\left(\frac{\omega}{\gamma}\right)_{\pm}^2 = \frac{2}{M} \left(\frac{\partial^2 F'}{\partial \theta_1^2} \pm \frac{\partial^2 F'}{\partial \theta_1 \partial \theta_2} \right) \times \left(\frac{2}{M \sin^2 \theta} \right) \left(\frac{\partial^2 F'}{\partial \phi_1^2} \pm \frac{\partial^2 F'}{\partial \phi_1 \partial \phi_2} \right), \quad (37)$$

with

$$\begin{aligned} \partial^2 F' / \partial \theta_1^2 &= \frac{1}{2} K_1 [2 \cos 4\theta + \sin^2 \theta (3 - 4 \sin^2 \theta)] \\ &\quad + \frac{1}{2} M H' \sin \theta + \pi M^2 N' \cos^2 \theta, \\ \partial^2 F' / \partial \theta_1 \partial \theta_2 &= \pi M^2 N' \cos^2 \theta, \\ \partial^2 F' / \partial \phi_1^2 &= -K_1 \sin^4 \theta + \frac{1}{2} M H' \sin \theta, \\ \partial^2 F' / \partial \phi_1 \partial \phi_2 &= 0. \end{aligned} \quad (38)$$

The plus and minus solutions correspond to excitation parallel and perpendicular to the domain walls. The susceptibility tensor elements are defined with reference to the following coordinate system (1,2,3): (1), normal to \mathbf{H} and in the plane of the disk; (2), perpendicular to the plane of the disk; (3) parallel to \mathbf{H} . The nonzero tensor elements are:

$$\begin{aligned} \chi_{11} &= \frac{4\pi M}{D_+} \left[\frac{2}{M \sin^2 \theta} \left(\frac{\partial^2 F'}{\partial \phi_1^2} + \frac{\partial^2 F'}{\partial \phi_1 \partial \phi_2} \right) \sin^2 \theta \right], \\ \chi_{22} &= \frac{4\pi M}{D_+} \left[\frac{2}{M} \left(\frac{\partial^2 F'}{\partial \theta_1^2} + \frac{\partial^2 F'}{\partial \theta_1 \partial \theta_2} \right) \right], \\ j\kappa_{12} = j\kappa_{21} = j\kappa &= \frac{4\pi M}{D_+} \left(\frac{j\omega_0}{\gamma} + \frac{1}{\gamma T} \right) \sin \theta, \\ \chi_{33} &= \frac{4\pi M}{D_-} \left[\frac{2}{M \sin^2 \theta} \left(\frac{\partial^2 F'}{\partial \phi_1^2} - \frac{\partial^2 F'}{\partial \phi_1 \partial \phi_2} \right) \cos^2 \theta \right], \end{aligned} \quad (39)$$

where

$$D_{\pm} = \left(\frac{\omega}{\gamma}\right)_{\pm}^2 - \left(\frac{\omega_0}{\gamma}\right)^2 + \frac{1}{\gamma^2 T^2} + j \frac{2\omega_0}{\gamma T}. \quad (40)$$

For rf propagation in direction 2 and surface excitation in direction 1, the cavity perturbation is given by (10). Hence the perturbation of the cavity depends upon:

$$\begin{aligned} &\frac{(1 + \chi_{11})(1 + \chi_{22}) - \kappa^2}{1 + \chi_{22}} \\ &= 1 + \frac{4\pi M \left[\frac{2}{M \sin^2 \theta} \left(\frac{\partial^2 F'}{\partial \phi_1 \partial \phi_2} \right) + 4\pi M \right] \sin^2 \theta}{\left(\frac{\omega}{\gamma}\right)_{+}^2 - \left(\frac{\omega_0}{\gamma}\right)^2 + \frac{1}{\gamma^2 T^2} + j \frac{2\omega_0}{\gamma T}}, \end{aligned} \quad (41)$$

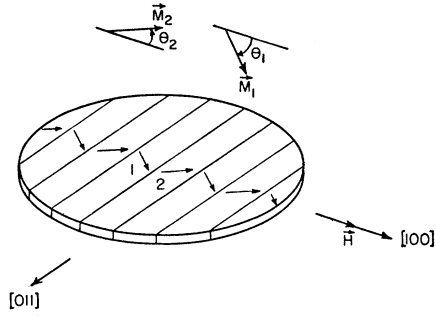


Fig. 5. Multidomain structure in cubic crystal of negative anisotropy. \mathbf{H} in $[100]$ direction of disk in $(01\bar{1})$ plane.

where

$$\begin{aligned} \left(\frac{\omega}{\gamma}\right)_{\pm}^2 &= \left[\frac{2}{M \sin^2 \theta} \left(\frac{\partial^2 F'}{\partial \phi_1^2} + \frac{\partial^2 F'}{\partial \phi_1 \partial \phi_2} \right) + 4\pi M \right] \\ &\quad \times \frac{2}{M} \left(\frac{\partial^2 F'}{\partial \theta_1^2} + \frac{\partial^2 F'}{\partial \theta_1 \partial \theta_2} \right). \end{aligned} \quad (42)$$

For propagation in direction 2 and excitation along 3, the cavity perturbation (see Appendix) depends upon $1 + \chi_{33}$.

(b) Disk in $(01\bar{1})$ Plane— \mathbf{H} in $[100]$ Direction

There are four easy axes of magnetization nearest the $[100]$ direction of an $(01\bar{1})$ surface. Two of these lie in the $(01\bar{1})$ plane, two in a plane perpendicular to it. When a sufficiently high field is applied in the $[100]$ direction, the magnetic structure would be expected to consist largely of two types of domains in which the magnetizations lie in the plane of the disk. See Fig. 5. Using the same nomenclature as in part (a), the free energy is

$$\begin{aligned} F &= \frac{1}{8} K_1 [\sin^2(2\theta_1) + \sin^4 \theta_1 \sin^2(2\phi_1) + \sin^2(2\theta_2) \\ &\quad + \sin^4 \theta_2 \sin^2(2\phi_2)] - \frac{1}{2} M H [\cos \theta_1 + \cos \theta_2] + \frac{1}{2} \pi M^2 \\ &\quad \times \left[(1 - 2n) \{ \sin \theta_1 \cos(\frac{1}{4}\pi + \phi_1) + \sin \theta_2 \cos(\frac{1}{4}\pi + \phi_2) \}^2 \right. \\ &\quad \left. + n (\cos \theta_1 + \cos \theta_2)^2 \right. \\ &\quad \left. + n \{ \sin \theta_1 \sin(\frac{1}{4}\pi + \phi_1) + \sin \theta_2 \sin(\frac{1}{4}\pi + \phi_2) \}^2 \right. \\ &\quad \left. + \frac{1}{2} \pi M^2 N [\cos \theta_1 - \cos \theta_2]^2 \right]. \end{aligned} \quad (43)$$

The equilibrium conditions are satisfied by $\theta_1 = \theta_2 = \theta$, $\phi_1 = \frac{1}{4}\pi$, $\phi_2 = 5\pi/4$, and

$$H = -(K_1/M) \cos \theta (2 - 3 \sin^2 \theta) + 4\pi M n \cos \theta. \quad (44)$$

The internal field is $H' = H - 4\pi M n \cos \theta$. The second-order derivatives are

$$\begin{aligned} \partial^2 F' / \partial \theta_1^2 &= \frac{1}{2} K_1 [2 \cos 4\theta + \sin^2 \theta (3 - 4 \sin^2 \theta)] \\ &\quad + \frac{1}{2} M H' \cos \theta + \pi M^2 N' \sin^2 \theta, \\ \partial^2 F' / \partial \theta_1 \partial \theta_2 &= -\pi M^2 N' \sin^2 \theta, \\ \partial^2 F' / \partial \phi_1^2 &= -K_1 \sin^4 \theta, \\ \partial^2 F' / \partial \phi_1 \partial \phi_2 &= 0, \end{aligned} \quad (45)$$

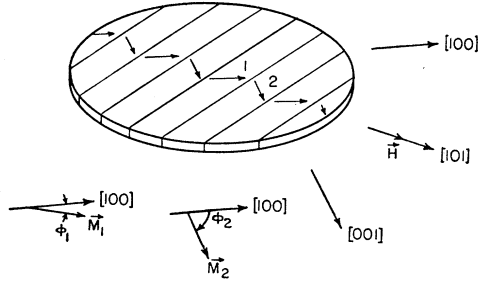


FIG. 6. Multidomain structure in cubic crystal of positive anisotropy. \mathbf{H} in $[101]$ direction of disk in (010) plane.

Here, the plus and minus solutions (37) correspond, respectively, to microwave excitation perpendicular and parallel to the domain walls. The nonzero tensor elements are

$$\begin{aligned}\chi_{11} &= \frac{4\pi M}{D_-} \frac{2}{M \sin^2\theta} \left(\frac{\partial^2 F'}{\partial \phi_1^2} - \frac{\partial^2 F'}{\partial \phi_1 \partial \phi_2} \right) \cos^2\theta, \\ \chi_{22} &= \frac{4\pi M}{D_-} \frac{2}{M} \left(\frac{\partial^2 F'}{\partial \theta_1^2} - \frac{\partial^2 F'}{\partial \theta_1 \partial \theta_2} \right), \\ j\kappa_{12} &= j\kappa_{21} = j\kappa = \frac{4\pi M}{D_-} \left(j \frac{\omega_0}{\gamma} + \frac{1}{\gamma T} \right) \cos\theta, \\ \chi_{33} &= \frac{4\pi M}{D_+} \frac{2}{M \sin^2\theta} \left(\frac{\partial^2 F'}{\partial \phi_1^2} + \frac{\partial^2 F'}{\partial \phi_1 \partial \phi_2} \right) \sin^2\theta,\end{aligned}\quad (46)$$

where D_{\pm} is given by (40). For rf propagation in direction 2 and surface excitation along 1, the cavity perturbation depends upon

$$\begin{aligned}\frac{(1+\chi_{11})(1+\chi_{22})-\kappa^2}{1+\chi_{22}} &= 1 \\ &+ \frac{4\pi M \left[\frac{2}{M \sin^2\theta} \left(\frac{\partial^2 F'}{\partial \phi_1^2} - \frac{\partial^2 F'}{\partial \phi_1 \partial \phi_2} \right) + 4\pi M \right] \cos^2\theta}{\left(\frac{\omega}{\gamma} \right)^2 - \left(\frac{\omega_0}{\gamma} \right)^2 + \frac{1}{\gamma^2 T^2} + j \frac{2\omega_0}{\gamma T}},\end{aligned}\quad (47)$$

where

$$\begin{aligned}\left(\frac{\omega}{\gamma} \right)^2_{\pm} &= \left\{ \frac{2}{M \sin^2\theta} \left(\frac{\partial^2 F'}{\partial \phi_1^2} - \frac{\partial^2 F'}{\partial \phi_1 \partial \phi_2} \right) + 4\pi M \right\} \\ &\times \frac{2}{M} \left(\frac{\partial^2 F'}{\partial \theta_1^2} - \frac{\partial^2 F'}{\partial \theta_1 \partial \theta_2} \right).\end{aligned}\quad (48)$$

For propagation in direction 2 and excitation along 3, the cavity perturbation depends upon $1+\chi_{33}$.

Cubic Crystals of Positive Anisotropy

Disk in (010) Plane— \mathbf{H} in $[101]$ Direction

Since the $[100]$ and $[001]$ directions are easy directions of magnetization, a structure similar to that of

Fig. 6 is expected for moderate values of \mathbf{H} . Using the nomenclature of $\Pi(b)$,

$$\begin{aligned}F &= \frac{1}{8} K_1 [\sin^2(2\theta_1) + \sin^4\theta_1 \sin^2(2\phi_1) \\ &+ \sin^2(2\theta_2) + \sin^4\theta_2 \sin^2(2\phi_2)] \\ &- \frac{1}{2} M H [\sin\theta_1 \cos(\frac{1}{4}\pi - \phi_1) + \sin\theta_2 \cos(\frac{1}{4}\pi - \phi_2)] \\ &+ \frac{1}{2} \pi M^2 \left[\frac{n(\sin\theta_1 \cos\phi_1 + \sin\theta_2 \cos\phi_2)^2}{+ n(\sin\theta_1 \sin\phi_1 + \sin\theta_2 \sin\phi_2)^2} \right] \\ &+ \frac{1}{2} \pi M^2 N [\sin\theta_1 \cos(\frac{1}{4}\pi - \phi_1) \\ &- \sin\theta_2 \cos(\frac{1}{4}\pi - \phi_2)]^2.\end{aligned}\quad (49)$$

Equilibrium is obtained for $\theta_1 = \theta_2 = \pi/2$, $\phi = \phi_1 = \pi/2 - \phi_2$ and

$$H = \frac{K_1 \sin 4\phi}{2M \sin(\frac{1}{4}\pi - \phi)} + 4\pi M n \cos(\frac{1}{4}\pi - \phi).\quad (50)$$

The internal field is $H' = H - 4\pi M n \cos(\frac{1}{4}\pi - \phi)$. The second-order derivatives are

$$\begin{aligned}\partial^2 F' / \partial \theta_1^2 &= \frac{1}{2} K_1 [2 - \sin^2 2\phi] + \frac{1}{2} M H' \cos(\frac{1}{4}\pi - \phi), \\ \partial^2 F' / \partial \theta_1 \partial \theta_2 &= 0, \\ \partial^2 F' / \partial \phi_1^2 &= K_1 \cos 4\phi + \frac{1}{2} M H' \cos(\frac{1}{4}\pi - \phi) \\ &+ \pi M^2 N' \sin^2(\frac{1}{4}\pi - \phi), \\ \partial^2 F' / \partial \phi_1 \partial \phi_2 &= \pi M^2 N' \sin^2(\frac{1}{4}\pi - \phi).\end{aligned}\quad (51)$$

The plus and minus solutions for $(\omega/\gamma)'$, Eq. (37) correspond, respectively, to excitation parallel and perpendicular to the domain walls. The nonzero tensor elements are

$$\begin{aligned}\chi_{11} &= \frac{4\pi M}{D_+} \frac{2}{M} \left(\frac{\partial^2 F'}{\partial \theta_1^2} + \frac{\partial^2 F'}{\partial \theta_1 \partial \theta_2} \right) \sin^2(\frac{1}{4}\pi + \phi), \\ \chi_{22} &= \frac{4\pi M}{D_+} \frac{2}{M} \left(\frac{\partial^2 F'}{\partial \phi_1^2} + \frac{\partial^2 F'}{\partial \phi_1 \partial \phi_2} \right), \\ j\kappa_{12} &= j\kappa_{21} = j\kappa = \frac{4\pi M}{D_+} \left(j \frac{\omega_0}{\gamma} + \frac{1}{\gamma T} \right) \sin(\frac{1}{4}\pi + \phi), \\ \chi_{33} &= \frac{4\pi M}{D_-} \frac{2}{M} \left(\frac{\partial^2 F'}{\partial \theta_1^2} - \frac{\partial^2 F'}{\partial \theta_1 \partial \theta_2} \right) \sin^2(\frac{1}{4}\pi - \phi),\end{aligned}\quad (52)$$

where D_{\pm} is given by (40). For propagation in direction 2 and excitation along 1 the cavity perturbation depends upon

$$\begin{aligned}\frac{(1+\chi_{11})(1+\chi_{22})-\kappa^2}{1+\chi_{22}} &= 1 \\ &+ \frac{4\pi M \left[\frac{2}{M} \left(\frac{\partial^2 F'}{\partial \theta_1^2} + \frac{\partial^2 F'}{\partial \theta_1 \partial \theta_2} \right) + 4\pi M \right] \sin^2(\frac{1}{4}\pi + \phi)}{\left(\frac{\omega}{\gamma} \right)^2_{+} - \left(\frac{\omega_0}{\gamma} \right)^2 + \frac{1}{\gamma^2 T^2} + j \frac{2\omega_0}{\gamma T}},\end{aligned}\quad (53)$$

where

$$\left(\frac{\omega}{\gamma}\right)_{\pm}^2 = \left[\frac{2}{M} \left(\frac{\partial^2 F'}{\partial \theta_1^2} + \frac{\partial^2 F'}{\partial \theta_1 \partial \theta_2} \right) + 4\pi M \right] \times \frac{2}{M \sin^2 \theta} \left(\frac{\partial^2 F'}{\partial \phi_1^2} + \frac{\partial^2 F'}{\partial \phi_1 \partial \phi_2} \right). \quad (54)$$

For propagation in direction 2 and excitation along 3, the cavity perturbation depends upon $1 + \chi_{33}$.

Uniaxial Crystals

(a) *Disk in Plane Containing [00·1] Axis—H in This Plane and Normal to [00·1] Axis*

As indicated in Fig. 7, a simple multidomain structure may be expected under these circumstances. If angles are defined as in II(c), the free energy per unit volume is

$$F = \frac{1}{2} K_1 [\sin^2 \theta_1 + \sin^2 \theta_2] - \frac{1}{2} M H [\sin \theta_1 \cos \phi_1 + \sin \theta_2 \cos \phi_2] + \frac{1}{2} \pi M^2 [n (\cos \theta_1 + \cos \theta_2)^2 + n (\sin \theta_1 \cos \phi_1 + \sin \theta_2 \cos \phi_2)^2 + (1 - 2n) (\sin \theta_1 \sin \phi_1 + \sin \theta_2 \sin \phi_2)^2] + \frac{1}{2} \pi M^2 N \times [\sin \theta_1 \cos \phi_1 - \sin \theta_2 \cos \phi_2]^2. \quad (55)$$

Equilibrium is achieved for $\theta = \theta_1 = \pi - \theta_2$, $\phi_1 = \phi_2 = 0$, and

$$H = [(2K_1/M) + 4\pi M n] \sin \theta. \quad (56)$$

The internal field is $H' = H - 4\pi M n \sin \theta$. The second-order derivatives are

$$\begin{aligned} \partial^2 F' / \partial \theta_1^2 &= K_1 \cos 2\theta + \frac{1}{2} M H' \sin \theta + \pi M^2 N' \cos^2 \theta, \\ \partial^2 F' / \partial \theta_1 \partial \theta_2 &= \pi M^2 N' \cos^2 \theta, \\ \partial^2 F' / \partial \phi_1^2 &= \frac{1}{2} M H' \sin \theta, \end{aligned} \quad (57)$$

$$\partial^2 F' / \partial \phi_1 \partial \phi_2 = 0.$$

The plus and minus values of $(\omega/\gamma)'$, Eq. (37), correspond, respectively, to excitation parallel and perpendicular to the domain walls. The tensor elements and the cavity perturbation relations follow from (39) through (42).

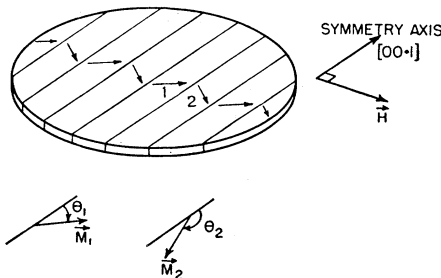


FIG. 7. Multidomain structure in uniaxial crystal. Disk in plane containing [00·1] axis. \mathbf{H} in this plane and normal to [00·1] axis.

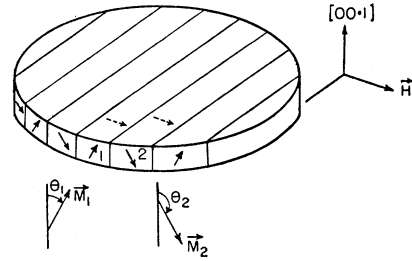


FIG. 8. Multidomain structure in uniaxial crystal. Disk and \mathbf{H} in (00·1) plane.

(b) *Disk and H in (00·1) Plane*

The domains will be assumed to be thin sheets whose planes are perpendicular to \mathbf{H} . This structure, depicted in Fig. 8, is the same as that proposed by Smit and Beljers² for $\text{BaFe}_{12}\text{O}_{19}$ under similar experimental conditions. If θ_1 and θ_2 are the inclination of the magnetizations measured from the symmetry axis and ϕ_1 and ϕ_2 are the azimuths measured from the direction of \mathbf{H} , the free energy is

$$F = \frac{1}{2} K_1 [\sin^2 \theta_1 + \sin^2 \theta_2] - \frac{1}{2} M H [\sin \theta_1 \cos \phi_1 + \sin \theta_2 \cos \phi_2] + \frac{1}{2} \pi M^2 \left[\begin{aligned} &n (\sin \theta_1 \sin \phi_1 + \sin \theta_2 \sin \phi_2)^2 \\ &+ n (\sin \theta_1 \cos \phi_1 + \sin \theta_2 \cos \phi_2)^2 \\ &+ (1 - 2n) (\cos \theta_1 + \cos \theta_2)^2 \end{aligned} \right] + \frac{1}{2} \pi M^2 N [\sin \theta_1 \cos \phi_1 - \sin \theta_2 \cos \phi_2]^2. \quad (58)$$

Equilibrium exists for $\theta = \theta_1 = \pi - \theta_2$, $\phi_1 = \phi_2 = 0$ and H given by (55). The internal field $H' = H - 4\pi M n \sin \theta$. The energy derivatives are given by (56). The $(\omega/\gamma)_{\pm}'$ solutions, (37), correspond, respectively, to excitation parallel and perpendicular to the domain walls. The tensor components and cavity perturbation formulas follow from Eqs. (52), (53), and (54).

IV. EXPERIMENTAL RESULTS

The magnetic structure in the (010) face of iron, a positive anisotropy crystal, has been studied extensively. Domain patterns in Fe single crystals have been examined with powder pattern techniques by Williams, Bozorth, and Shockley¹⁴ and by Bates and collaborators.¹⁵ A theoretical analysis of the expected patterns has been given by Néel.¹⁶ Ferromagnetic resonance observations at 23.675 and 9.260 kMc/sec were made on a (010) face of a Si-Fe crystal by Kip and Arnold.⁸ They found the angular variation of resonance field at 23.675 kMc/sec to correspond to the Kittel formula. At the lower frequency, deviations from the expected angular variation and an additional resonance peak were noted. See Figs. 9 and 10. This secondary reso-

¹⁴ Williams, Bozorth, and Shockley, *Phys. Rev.* **75**, 155 (1949).

¹⁵ L. F. Bates and F. E. Neale, *Proc. Phys. Soc. (London)* **A63**, 374 (1950); L. F. Bates and C. D. Mee, *Proc. Phys. Soc. (London)* **A64**, 129 (1952).

¹⁶ L. Néel, *J. phys. radium* **5**, 241, 265 (1944).

nance was observed when the field was along a $[101]$ direction.

At the higher frequency, the relations given in Sec. II(b) apply. The value of H in relation to K_1/M is such that the angle between \mathbf{M} and \mathbf{H} is at most two degrees. Equations (23) and (24) can be used; no significant deviations from the Kittel formulas are expected. The 9.260-kMc/sec data are much more interesting. From the resonance field at ϕ equal to zero, the main resonance field point at $\phi=45^\circ$, and the value of $M=1575$ gauss/cm³ the following crystal parameters are derived:

$$K_1/M=193 \text{ oe}, \quad K_1=3.04 \times 10^5 \text{ ergs/cm}^3, \quad g=2.18.$$

The angular variation of resonance field predicted by (22) and these parameters is in accord with the experimental observations in Fig. 9. The explanation given by Kip and Arnold for the field deviation is essentially equivalent to this except that the distinction between \mathbf{H} and \mathbf{H}' and Φ and Φ' is not always clearly drawn.

The multidomain analysis of Sec. III provides a satisfactory explanation for the secondary resonance. From the experimental data and relations (50) and (54) ϕ is found to be $19^\circ 11'$, and N' is 4.59×10^{-2} . If the domain length L is much greater than the domain width w and microwave skin depth δ , N' is expected to equal $\delta/(\delta+w)$. The skin depth δ is given by

$$\delta = \left(\frac{2}{\omega_0 \sigma \mu_0} \right)^{\frac{1}{2}} \frac{1}{[(\mu_a''^2 + \mu_a'^2)^{\frac{1}{2}} + \mu_a'']^{\frac{1}{2}}},$$

where μ_a' and μ_a'' are the real and imaginary parts of (53). Using a ΔH of 400 oersteds, μ_a'' at resonance is found to be 270, δ is 1.67×10^{-5} cm and the value for w is then 3.47×10^{-4} cm. The magnitude of the secondary resonance peak relative to the primary is about one-half the expected value. (See Fig. 10.) This can be accounted for by a spread in domain spacing of $\pm 30\%$ about the center value 3.47×10^{-4} cm, a not unlikely result. The value of w predicted by Néel's formula in the central portion of the disk is about one-seventh the microwave value. This is not too disturbing since

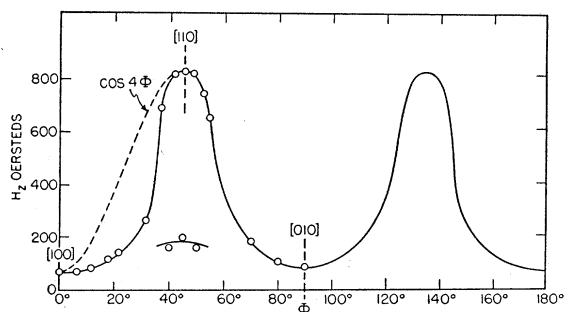


FIG. 9. Resonance magnetic field vs angle between applied field and $[100]$ direction in Fe crystal, where frequency is 9.260 kMc/sec—adapted from Kip and Arnold, reference 8.

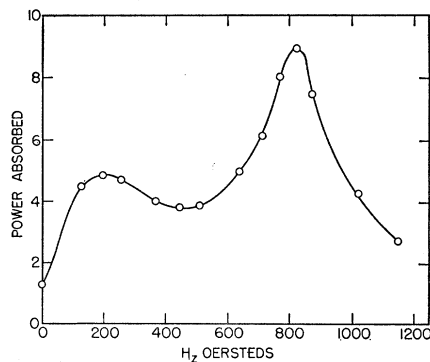


FIG. 10. Resonance absorption curve at 9.260 kMc/sec showing double peak which occurs when Φ is near 45° —adapted from Kip and Arnold, reference 8.

powder-pattern observations^{14,15} have only confirmed Néel's theory qualitatively. Apparently it is very difficult to obtain a specimen fulfilling the ideal conditions considered by Néel. Williams *et al.*,¹⁴ for instance, observed spacings five times as large as expected. Bates and Neale¹⁵ observed spacings in closer agreement with the theory, but did not find the spacings to be proportional to $L^{\frac{1}{2}}$ as predicted by Néel. Bates and Mee¹⁵ found the $L^{\frac{1}{2}}$ formula to be valid but found the domain widths to be four times larger than anticipated. The theoretical formula was derived for a rectangular specimen; the domains of closure at the edges of the circular sample used by Kip and Arnold may be modified sufficiently to account for the observed discrepancies. Finally, Kip and Arnold give evidence indicating that the crystal surface was strained. They felt that the effects of strain played a minor role in the resonances, this may not be true in the multidomain region. In summary, the Kip and Arnold data are in reasonable agreement with the concepts presented in this paper. Curves of resonance frequency vs magnetic field for the single and multidomain regions are shown in Fig. 11. The numerical data correspond to that of Figs. 9 and 10.

Powder-pattern domain observations on $(01\bar{1})$ surfaces of negative anisotropy crystals have been made by Bozorth and Walker,¹⁷ Williams and Walker,¹⁸ and by Bates and Wilson.¹⁹ Bozorth and Walker investigated the patterns found when \mathbf{H} was applied along a $[011]$ direction of a 60-40 Co-Ni crystal. Williams and Walker saw similar patterns in a pure Ni specimen, reporting spacings of the order of 10^{-2} cm. Microwave investigations of these particular structures have not been reported. Bates and Wilson¹⁹ found spacings of the order of 10^{-3} cm when \mathbf{H} was applied along the $[100]$ direction of an $(01\bar{1})$ Ni specimen. Bates and

¹⁷ R. M. Bozorth and J. G. Walker, Phys. Rev. **79**, 888 (1950).

¹⁸ H. J. Williams and J. G. Walker, Phys. Rev. **83**, 634 (1951).

¹⁹ L. F. Bates and G. W. Wilson, Proc. Phys. Soc. (London) **A66**, 819 (1953).

Wilson suggested that the Ni domain structure corresponded closely to that proposed by Néel for (010) Fe specimens but did not attempt domain width calculations. Reich⁹ has recently investigated ferromagnetic resonance in (011) plane nickel specimens at temperatures ranging down to 77°K at 9.00 kMc/sec and 4.2°K at 24.30 kMc/sec. At 9.00 kMc/sec Reich observed secondary resonances in the [100] direction at low temperatures. The specimens used at 9.00 kMc/sec were in the form of strip-line resonators. The crystal orientations of these strips and the design of the apparatus did not permit resonance observations in the [011] direction. Interpretation of the secondary resonance data is difficult since the [100] direction was not parallel to the axis of any of the strips. Calculations made from Reich's 130°K observations suggest a domain spacing of 5×10^{-6} cm but this must be regarded as highly speculative.

Ohtsuka¹⁰ has reported on ferromagnetic resonance absorption at 24.00 kMc/sec in magnetically uniaxial Co at temperatures ranging from 180° to 380°C. The dc magnetic field was applied parallel to the long axis of the rectangular specimens used. Since the crystal symmetry axis was not parallel to the specimen axis in any of the samples, Ohtsuka's data must be corrected for the inclination of \mathbf{M} to \mathbf{H} in a manner similar to that

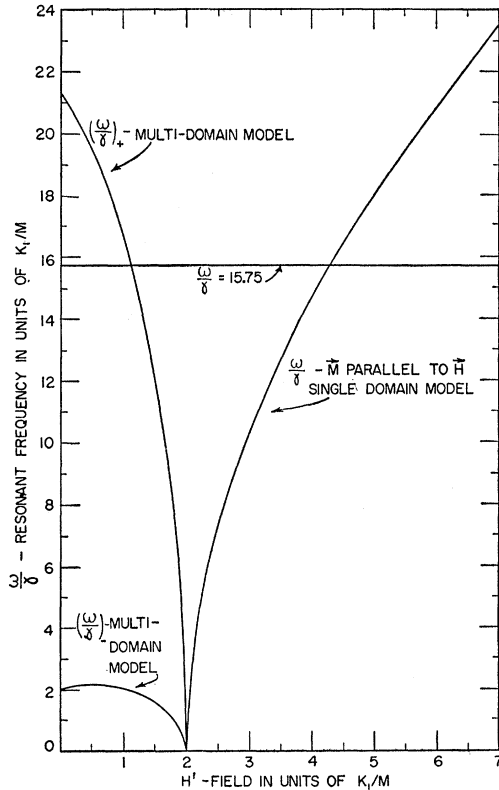


FIG. 11. Resonance frequency vs magnetic field curves at $\Phi=45^\circ$ computed from Kip and Arnold data.

of Sec. II(c). These calculations are extremely tedious and have not been attempted. The anisotropy constants and g values reported by Ohtsuka may require significant correction. Ohtsuka did not report any secondary resonance peaks. Other than those observed by Williams,¹¹ no Co domain patterns have been reported in the literature.

Smit and Beljers, in their work on $\text{BaFe}_{12}\text{O}_{19}$,² observed ferromagnetic resonance in a multidomain structure when the microwave field was *perpendicular* to the domain walls. No such resonance has yet been observed in any other ferromagnetic substance. As can be ascertained from the example of Fig. 11, these resonances occur at frequencies often far below those for which the microwave field lies parallel to the domain walls. Many of these ferromagnetic resonances are, in addition, very broad—this would make detection of the perpendicular field resonance difficult.

APPENDIX

Consider a medium specified by the microwave susceptibility tensor (2). The corresponding permeability tensor is obtained by adding unity to the diagonal elements, yielding

$$\begin{pmatrix} \mu_{11} & -j\kappa_{12} & 0 \\ j\kappa_{21} & \mu_{22} & 0 \\ 0 & 0 & \mu_{33} \end{pmatrix}. \quad (59)$$

For single-domain analysis, the coordinate system is defined as follows: (1), normal to \mathbf{M} and in the plane of the disk; (2), perpendicular to the plane of disk; (3), parallel to \mathbf{M} . For the simple types of multidomain structure considered in this paper, \mathbf{M} is replaced by \mathbf{H} in the above definitions. The microwave quantities \mathbf{b} and \mathbf{h} are then related as follows:

$$\begin{aligned} b_1 &= \mu_{11}h_1 - j\kappa_{12}h_2, \\ b_2 &= j\kappa_{21}h_1 + \mu_{22}h_2, \\ b_3 &= \mu_{33}h_3. \end{aligned} \quad (60)$$

For plane-wave solutions of Maxwell's equations for a highly conductive medium, one has

$$\nabla \times \mathbf{e} = -(1/c)\partial \mathbf{b} / \partial t, \quad \nabla \times \mathbf{h} = (4\pi\sigma/c)\mathbf{e}, \quad (61)$$

$$\begin{aligned} \mathbf{b} &= \mathbf{b}_0 \exp[j\omega t - P(\mathbf{n} \cdot \mathbf{r})], \\ \mathbf{h} &= \mathbf{h}_0 \exp[j\omega t - P(\mathbf{n} \cdot \mathbf{r})], \end{aligned} \quad (62)$$

$$\mathbf{e} = \mathbf{e}_0 \exp[j\omega t - P(\mathbf{n} \cdot \mathbf{r})],$$

and

$$\begin{aligned} \lambda \mathbf{b}_0 &= P^2[\mathbf{n}(\mathbf{n} \cdot \mathbf{h}_0) - \mathbf{h}_0], \\ \lambda c \mathbf{e}_0 &= -j\omega P[\mathbf{h}_0 \times \mathbf{n}], \end{aligned} \quad (63)$$

where

$$\lambda = -j\omega 4\pi\sigma/c^2.$$

For propagation into the metal, $n_1 = n_3 = 0$, $n_2 = 1$.

Two solutions are found from (63):

(1) Parallel excitation:

$$\begin{aligned} e_2 = e_3 = h_1 = h_2 = 0, \\ P_{11}^2 = -\lambda\mu_{33}, \\ e_1/h_3 = j\omega P_{11}/\lambda c. \end{aligned} \quad (64)$$

(2) Perpendicular excitation:

$$\begin{aligned} e_1 = e_2 = h_3 = 0, \\ h_2 = -j(\kappa_{21}/\mu_{22})h_1, \\ P_{\perp}^2 = -\lambda(\mu_{11}\mu_{22} - \kappa_{12}\kappa_{21})/\mu_{22}, \\ e_3/h_1 = -j\omega P_{\perp}/\lambda c. \end{aligned} \quad (65)$$

For rf excitation at the angle α to direction 3, the

cavity perturbation is

$$\begin{aligned} \Delta\left(\frac{1}{Q}\right) - 2j\frac{\Delta\omega_0}{\omega_0} \\ = \frac{c^2}{4\pi\omega_0\sigma}(P_{\perp}\sin\alpha + P_{11}\cos^2\alpha)\int h_k^2 ds, \end{aligned} \quad (66)$$

where \mathbf{h}_k is the normalized unperturbed field for the mode k in which the cavity is oscillating. If $1/Q_0$ is the real part of (66) when $\mu_{11} = \mu_{22} = \mu_{33} = 1$, $\kappa_{12} = \kappa_{21} = 0$, then

$$\Delta\left(\frac{1}{Q}\right) - 2j\frac{\Delta\omega_0}{\omega_0} = \frac{1}{Q_0} \frac{c}{(2\pi\omega_0\sigma)^{\frac{1}{2}}}(P_{\perp}\sin^2\alpha + P_{11}\cos^2\alpha). \quad (67)$$

The above analysis is an extension of that given by Young and Uehling.¹

Triple Acceptors in Germanium

H. H. WOODBURY AND W. W. TYLER

General Electric Research Laboratory, Schenectady, New York

(Received September 28, 1956)

Both copper and gold introduce three acceptor levels in the forbidden band of germanium. In addition to the levels at 0.04 eV and 0.32 eV from the valence band, Cu introduces a third acceptor level at 0.26 eV from the conduction band. Identification of these levels has been made for a series of samples in which the Cu concentration was varied from 10^{13} cm⁻³ to 2×10^{16} cm⁻³. Evidence is presented confirming Dunlap's observations that Au introduces a donor level 0.05 eV from the valence band and acceptor levels 0.15 eV from the valence band and 0.20 eV from the conduction band. In addition to these, Au also introduces a third acceptor level 0.04 eV from the conduction band. Studies of charged impurity scattering indicate that both Cu and Au sites may be triply charged by compensation. The observation that impurities with an s^1 configuration are triple acceptors is consistent with the hypothesis that the tendency to form tetrahedral bonds determines the acceptor action of impurities in Ge.

I. INTRODUCTION

ELEMENTS of the third column of the periodic table with a s^2p^1 configuration act as single acceptors in germanium introducing the familiar hydrogen-like states 0.01 eV from the valence band. Recent work on "deep level" impurities¹ has shown that elements with an s^2 configuration act as double-acceptor impurities in germanium. The assumption that such impurities are substitutional leads to the generalization that their acceptor action is determined by the tendency to complete the tetrahedral bonding arrangement with the four nearest neighbor germanium atoms. An extension of this generalization suggests that elements with an s^1 configuration might act as triple-acceptor impurities in germanium. Two impurity elements with an s^1 configuration, copper and gold, have been studied by several workers. However, published results show some disagreement and incompleteness.

¹ See W. W. Tyler and H. H. Woodbury, *Phys. Rev.* **102**, 647 (1956), and references quoted therein.

Early experiments² showed that copper diffuses rapidly in germanium, that it acts as an acceptor, and that it can account for many effects of heat treatment. An energy level associated with copper was observed at approximately 0.04 eV above the valence band in germanium.³⁻⁵ The existence of a deeper level was deduced from measurements of the lifetime of minority carriers in copper-doped germanium.⁶ The presence of such a level, near the center of the forbidden band, has been indicated by several workers employing various techniques.^{4,5,7} Battey and Baum clearly demonstrated the existence of this second acceptor level and located

² C. S. Fuller and J. D. Struthers, *Phys. Rev.* **87**, 526 (1952); W. P. Slichter and E. P. Kolb, *Phys. Rev.* **87**, 527 (1952).

³ F. J. Morin and J. P. Maita, *Phys. Rev.* **90**, 337(A) (1953).

⁴ W. C. Dunlap, Jr., *Phys. Rev.* **96**, 40 (1954).

⁵ Burstein, Davisson, Bell, Turner, and Lipson, *Phys. Rev.* **93**, 65 (1954); W. Kaiser and H. Y. Fan, *Phys. Rev.* **93**, 977 (1954).

⁶ Burton, Hull, Morin, and Severiens, *J. Phys. Chem.* **57**, 853 (1954).

⁷ H. B. Briggs, reported in reference 6. See also D. H. Rank and D. C. Cronmeyer, *Phys. Rev.* **90**, 202 (1953) for studies of "thermiated" germanium.